

Interiors of Giant Planets Inside and Outside the Solar System

Tristan Guillot

An understanding of the structure and composition of the giant planets is rapidly evolving because of (i) high-pressure experiments with the ability to study metallic hydrogen and define the properties of its equation of state and (ii) spectroscopic and in situ measurements made by telescopes and satellites that allow an accurate determination of the chemical composition of the deep atmospheres of the giant planets. However, the total amount of heavy elements that Jupiter, Saturn, Uranus, and Neptune contain remains poorly constrained. The discovery of extrasolar giant planets with masses ranging from that of Saturn to a few times the mass of Jupiter opens up new possibilities for understanding planet composition and formation. Evolutionary models predict that gaseous extrasolar giant planets should have a variety of atmospheric temperatures and chemical compositions, but the radii are estimated to be close to that of Jupiter (between 0.9 and 1.7 Jupiter radii), provided that they contain mostly hydrogen and helium.

Constraints on the interior structure of the giant planets of our solar system—Jupiter, Saturn, Uranus, and Neptune—are derived from knowledge of their mass M , equatorial radius a , and gravitational moments J_2 , J_4 , and J_6 . Measurements of these quantities go back to the Pioneer and Voyager spacecraft missions (1). Improvements in measurements of the gravitational moments of Saturn must await the arrival of the Cassini-Huygens mission in the saturnian system in 2004, and measurements for the other planets must await future space missions. The past years have nevertheless been rich in advances in giant planet research: Galileo measured the composition and structure of Jupiter's atmosphere with unprecedented accuracy (2), compression experiments succeeded in pressurizing hydrogen above a pressure of 10^{11} Pa (100 GPa, or 1 Mbar) (3, 4), and giant planets were discovered orbiting other stars (5). This review describes our present understanding of the internal structure of giant planets both inside and outside of our solar system.

At the foundation of any understanding of the interiors of the giant planets and brown dwarfs (6) lies knowledge about the behavior of chemical species at high pressures, and of hydrogen in particular, it being the most abundant element. At low pressures and temperatures, hydrogen is an insulator in the form of a strongly bound diatomic molecule. At high pressures (~ 100 GPa) and moderate temperatures ($\leq 10^5$ K), it dissociates and eventually ionizes to transform into an alkali metal. This form of hydrogen, called metallic

hydrogen, escaped detection for many years but has now been observed. Shock wave experiments with two-stage gas guns succeeded in measuring electrical conductivities of fluid hydrogen up to 180 GPa and 3000 K (3). In these experiments, an increase in the measured conductivity by four orders of magnitude was observed when pressure increased from 90 to 140 GPa. The conductivity then became constant, which was initially interpreted as a sign that metallic hydrogen had been formed. However, the conductivity was still smaller than theoretical estimates for a fully ionized hydrogen metal (7). In fact, the fluid still retained a strong pairing character at these pressures. Other experiments (4) used a high-intensity laser to compress deuterium to even greater pressures (300 GPa), but at higher temperatures (up to ~ 70000 K). The liquid was found to be more compressible than expected, and for the first time the hydrogen isotope was compressed to a fully dissociated, partially ionized, metallic fluid state. In both sets of experiments, no discontinuous behavior revealing a first-order insulator-metal transition was observed.

These results cannot yet be included in actual interior models of the giant planets without an appropriate equation of state, which still needs to be calculated. The last theoretical effort to model the behavior of hydrogen at high pressures in this astrophysical context, the widely used Saumon-Chabrier equation of state (8), agrees with the experiments at low and high pressures but needs to be improved in the 50 to 300 GPa (0.5 to 3 Mbar) region. Furthermore, it predicts the presence of a first-order (discontinuous) phase transition for temperatures up to 15300 K (the critical point), which is questioned by the experiments. Recent calcula-

tions (9) using softer interaction potentials, as indicated by the laser experiments, predict a lower critical temperature (by ~ 700 K). This would imply that the laser experiments are supercritical, whereas the gas-gun experiments have not attained a high enough pressure to reach the metallic phase. Laboratory results thus reveal that the hydrogen phase transition is even much more complex than previously thought, as molecules, atoms, protons, itinerant electrons, and even clusters (10) can coexist over an extended pressure range (100 to 300 GPa). The corresponding uncertainties on the predicted density profiles have to be included within interior model calculations (11).

Jupiter and Saturn

The interiors of Jupiter and Saturn have traditionally been divided into three distinct, quasi-homogeneous regions (12): a central dense ice and rock core, a fluid metallic hydrogen region, and (at pressures lower than about 100 GPa) a fluid molecular hydrogen shell. Spectroscopic and in situ measurements can only probe the upper levels of the planets' atmospheres, but the inferred chemical composition is generally thought to apply to the entire molecular region (after allowing for changes due to chemical reactions and condensation processes). In particular, Jupiter's and Saturn's atmospheres, and therefore their molecular regions, are believed to lack some of the helium that was present at their formation. Indeed, the helium mass mixing ratio Y , accurately measured in the jovian atmosphere by the Galileo probe, is such that $Y/(X + Y) = 0.238 \pm 0.007$ (13), X being the hydrogen mass mixing ratio. This value is lower than that in the protosolar nebula, for which it is inferred from solar models that $Y/(X + Y) = 0.280 \pm 0.005$ (14). Saturn's atmosphere probably has even less helium than Jupiter, as indicated by Voyager 2 data (15). Because there is no known physical process that can decrease the He/H ratio to this extent, the missing helium is believed to be hidden deeper inside the planets.

The removal of the atmospheric helium is explained by a H-He phase separation (16), by a first-order transition from molecular to metallic hydrogen (17), or by both. From the point of view of interior models, the presence of a helium-poor and a helium-rich region is at least as important as the molecular-to-metallic transition itself. This distinction between the two regions is needed to determine

Observatoire de la Côte d'Azur, Département Cassini, CNRS UMR 6529, Boîte Postale 4229, 06304 Nice Cedex 04, France. E-mail: guillot@obs-nice.fr

the amount of heavy elements (that is, any species other than hydrogen and helium) that the planets hold and has direct consequences for their evolution, as gravitational energy is transformed into heat during helium sedimentation (18). However, because any H-He phase separation is expected near the molecular-to-metallic transition of hydrogen (19), it is convenient to equate the helium-poor and helium-rich regions with the molecular and metallic regions, respectively.

Another important feature of present-day models of Jupiter and Saturn is the assumption that the molecular and metallic regions are quasi-homogeneous. This is because the planets emit significant intrinsic heat fluxes, and are therefore hot, fluid, and mainly convective (18, 20). The assumption probably breaks down at several locations (21), as follows: (i) Where a minimum in the mean radiative opacities of the fluid at temperatures of 1300 to 1800 K (22) probably yields the presence of a radiative region in Jupiter and possibly Saturn (23). In such a radiative zone, a variation of chemical abundance is in principle possible, either through gravitational settling or through the slow mixing of material that struck the planet after its formation. Gravitational settling is expected to be small because it is inhibited by turbulent diffusion (24). Helium (and tentatively any late supply of heavy elements to the outermost layers) should be able to sink through the radiative zone thanks to a salt-finger type of instability (25), thus ensuring an almost uniform chemical composition of the radiative zone. (ii) In the region of varying helium concentration, in which convection may be suppressed. The extent of this inhomogeneous region (Fig. 1) is estimated from fully ionized phase separation models (19). In reality, the inhomogeneous region could be narrower or wider. It is not included in any interior models so far, but this seems justified because the gravitational moments only provide constraints on quantities that are averaged over relatively extended regions. More important, this region could be a relatively efficient barrier to the mixing of minor species, because they would have to be transported by slow diffusion processes. The same would occur at the boundary of a first-order transition from the molecular to the metallic phase (18).

Interior models of Jupiter and Saturn are calculated by solving the standard quasi-hydrostatic differential equations, including the rotational potential calculated within the theory of figures (26). In recent calculations, only models that match all observational constraints are considered. Uncertainties in the equation of state, surface temperature, opacities, internal rotation, and observational error bars on the gravitational moments are taken into account to determine the allowed range of internal compositions of these planets. The

space of parameters is then extensively studied within the three-layer assumption. Additional constraints are provided by planetary evolution calculations, because they should yield model ages that are in agreement with that of the solar system (23). A critical improvement of the evolutionary models lies in the ability to account for helium differentiation, because it can considerably slow down the contraction and cooling of a given planet (27). In fact, helium sedimentation is required to explain Saturn's intrinsic heat flux and may be significant in Jupiter as well. The characteristics of typical Jupiter and Saturn models are shown in Fig. 1, including corresponding uncertainties in the temperature profiles.

The resulting constraints on the enrichment in heavy elements of Jupiter and Saturn's metallic regions relative to solar composition (Fig. 2) are weak. However, the enrichments of the molecular regions can be usefully compared to other observations. Galileo probe measurements are compatible with an enrichment of Jupiter's deep atmosphere [pressure (P) ≥ 15 bar] of two to four times the solar values in C, N, and S (28). The Galileo probe results are thus consistent with an abundance of major gases [except helium, neon (16), and water] that is two to four times larger than in the sun, which is in agreement with interior models using the new helium mixing ratio but not the one derived from Voyager data (Fig. 2). The lack of abundant water in the Galileo measurements is thought to be due to jovian meteorology, and its bulk

abundance is therefore still unknown (28, 29). On the basis of the Galileo measurements, interior models also rule out water abundances larger than 10 times solar in Jupiter's deep atmosphere. In Saturn, spectroscopic measurements indicate enrichments of CH_4 on the order of three to five times solar (30). The lower measured abundance of NH_3 (Fig. 2) is certainly due to condensation, because the planet is cooler than Jupiter. The global enrichments calculated with the Voyager helium mass mixing ratio (15) are incompatible with the observed CH_4 abundance (Fig. 2). Instead, static and evolutionary models favor a higher value of $Y/(X + Y) = 0.11 - 0.25$ (23, 27).

Table 1 gives the total mass of heavy elements in Jupiter and Saturn and shows how they are distributed as core mass in the metallic and molecular envelopes. It is not required that Jupiter have a central core in order to fit the gravitational moments, but that solution is not the preferred one because it implies a rather extreme equation of state and also yields high heavy-element enrichments (in the upper range of Fig. 2). In any case, Jupiter's core must be smaller than 10 Earth masses (M_{\oplus}). Furthermore, it is generally found that Saturn has a bigger core than Jupiter, but the constraints are relatively weak because some of the material in the deep metallic envelope could be accounted for as core mass, and vice versa. It is important to note that heavy elements in Jupiter's and Saturn's molecular regions, and some of those in their metallic regions, were probably

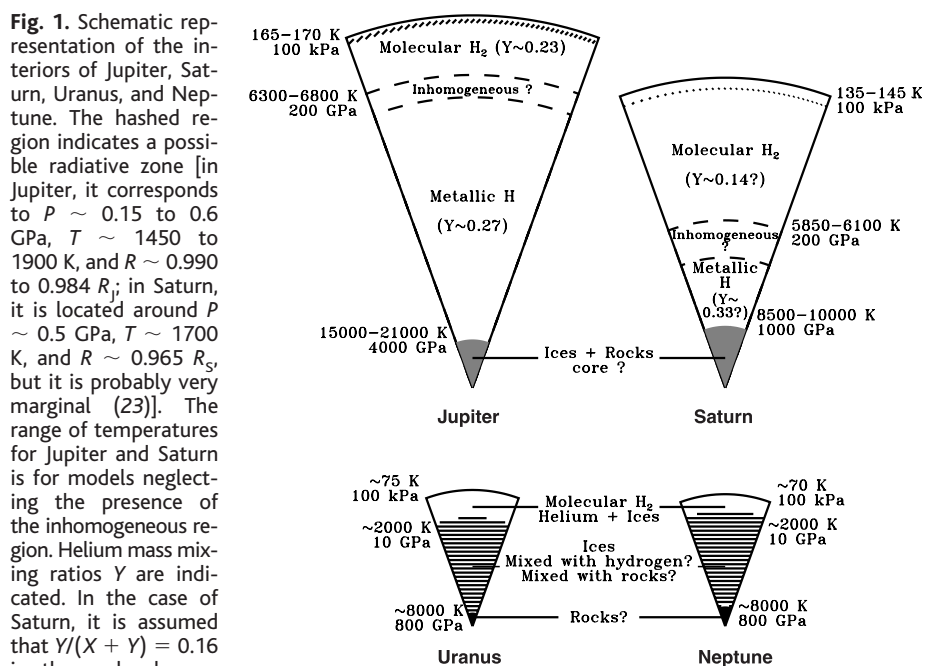


Fig. 1. Schematic representation of the interiors of Jupiter, Saturn, Uranus, and Neptune. The hashed region indicates a possible radiative zone [in Jupiter, it corresponds to $P \sim 0.15$ to 0.6 GPa, $T \sim 1450$ to 1900 K, and $R \sim 0.990$ to $0.984 R_J$; in Saturn, it is located around $P \sim 0.5$ GPa, $T \sim 1700$ K, and $R \sim 0.965 R_S$, but it is probably very marginal (23)]. The range of temperatures for Jupiter and Saturn is for models neglecting the presence of the inhomogeneous region. Helium mass mixing ratios Y are indicated. In the case of Saturn, it is assumed that $Y/(X + Y) = 0.16$ in the molecular region. The size of the central rock and ice cores of Jupiter and Saturn is very uncertain (see text). Two representative models of Uranus and Neptune are shown, but their actual interior structure may be significantly different (34). The figure is adapted and updated from (19).

brought in after their formation (after they had captured most of their hydrogen and helium). It is as yet unclear whether material was exchanged between the molecular and metallic regions. Models of giant planet formation should account for the planetesimals captured during and after formation (31).

Uranus and Neptune

The structure of the “ice giants” Uranus and Neptune is more difficult to grasp, notably because they contain a relatively smaller fraction of hydrogen and helium, and because their gravitational moments are known with a lower accuracy. Spectroscopic measurements indicate that their hydrogen-helium atmospheres contain a large proportion of heavy elements, mainly CH_4 , which is enriched by a factor of ~ 30 as compared to solar composition (32). The two planets have similar masses ($14.53 M_{\oplus}$ for Uranus and $17.14 M_{\oplus}$ for Neptune) and radii. Neptune’s larger mean density is partly due to greater compression but could also be the result of a slightly different composition. The gravitational moments require that the density profiles lie close to that of “ice” (a mixture initially composed of H_2O , CH_4 , and NH_3 but whose composition most probably does not consist of intact molecules in the planetary interior), except in the outermost layers, which have a density closer to that of hydrogen and helium (33). Three-layer models of Uranus and Neptune consisting of a central “rock” core (magnesium-silicate and iron material), an ice layer, and a hydrogen-helium gas envelope have been calculated (Fig. 1) (34).

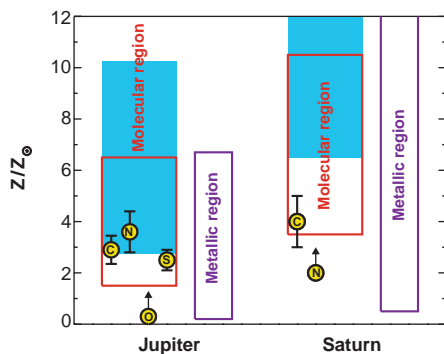


Fig. 2. Constraints on the mass mixing ratio of heavy elements, in solar units [assuming the mass mixing ratio of heavy elements in the sun (Z_{\odot}) = 0.0192 (58)] of the molecular (red rectangles) and metallic (purple rectangles) regions of Jupiter and Saturn. The helium mixing ratios used for the calculation are the Galileo value for Jupiter (13) and $Y/(Y + X) = 0.16 \pm 0.05$ for Saturn (see text). The enrichments in the molecular regions that would have been found with the old Voyager values (13, 15) are indicated by blue areas. When available, the observed abundances of C, N, O, and S are indicated. The maximum value for the heavy element enrichment of Saturn’s metallic region is $20 Z_{\odot}$.

The fact that models of Uranus assuming homogeneity of each layer and adiabatic temperature profiles fail to reproduce its gravitational moments seems to imply that substantial parts of the planetary interior are not homogeneously mixed (35). This could explain the fact that Uranus’ heat flux is so small: Its heat would not be allowed to escape to space by convection but through a much slower diffusive process in the regions with a high molecular weight gradient. Such regions would also be present in Neptune but much deeper, thus allowing more heat to be transported outward. The existence of these non-homogeneous partially mixed regions is further confirmed by the fact that if hydrogen is supposed to be confined solely to the hydrogen-helium envelope, models predict ice/rock ratios on the order of 10 or more, which is much larger than the protosolar value of ~ 2.5 . On the other hand, if we impose the constraint that the ice/rock ratio be protosolar, the overall composition of both Uranus and Neptune is, by mass, about 25% rock, 60 to 70% ice, and 5 to 15% hydrogen and helium (34, 35).

The Radii of Extrasolar Giant Planets

The discovery of planets outside our solar system represents an opportunity to learn even more about the formation of planets in general and to determine how unique our solar system may be. Although the present constraints on the interior structures of Jupiter, Saturn, Uranus, and Neptune are weak, obtaining the characteristics of extrasolar giant planets with different masses and orbital parameters will enlighten us about their composition. Measurements of radii are within reach, most notably with programs designed to detect planetary transits by photometry (through the slight dimming of a star when an orbiting planet happens to cross the line of sight) (36). The radius of a planet is a function of its mass, age, degree of insolation by the parent star, and composition (37). Let us suppose that the mass is accurately known (for example, by the combination of transit detection and radial velocity measurements) and that the age and albedo can be independently estimated. For a given helium/hydrogen ratio, the amount of heavy elements in the planet can then be determined.

The radii of extrasolar giant planets can be

Table 1. Amount of heavy elements (in M_{\oplus}) in Jupiter and Saturn.

Region	Jupiter	Saturn
Core	0–10	6–17
Molecular region	1.6–6.1	2.8–8.8
Metallic region	0.7–34	0–17
Total	11–42	19–31
(core + envelope)		

predicted with the same equations that govern the evolution of stars. The evolution of giant planets in isolation or relatively far from their parent star has been studied extensively and now includes detailed treatments of the atmosphere (38). These calculations can be extended to planets orbiting close to their stars (39), with a lesser precision because of uncertainties about how much of the incoming stellar light is absorbed by the planetary atmosphere. Figure 3 gives examples of effective temperatures and radii predicted for some of the recently found extrasolar giant planets and brown dwarfs, assuming solar composition and a factor of 2 uncertainty on the mass (due to the fact that radial velocity measurements only yield $M \sin i$, where i is the inclination of the orbital plane), and including uncertainties on the age (40) and albedo (between 0.1 and 0.5). It illustrates the diversity of planets detected so far. Because of the range of temperatures, many different condensates (from ammonia to silicates) are expected in planetary atmospheres (41, 42). However, the calculated radii are always close to that of Jupiter, until the mass is large enough to sustain hydrogen fusion, at about 75 Jupiter masses (M_J) (38, 43). A local maximum of the radius at a mass of $\sim 4 M_J$ for isolated planets is due to the competition between additional volume and increased gravity. (This is because, when considering planets of larger masses, the degenerate metallic hydrogen region grows at the expense of the molecular region.) Planets that are significantly heated by their star have larger radii for smaller masses because the outermost layers are substantially puffed up when gravity is small.

An important feature of giant planets at close orbital distances, or “hot Jupiters,” is that they have already entered an evolutionary stage in which they become progressively more radiative (that is, less convective), as they strive to attain complete equilibrium with the star (ideally, they will eventually become isothermal). This will also happen for planets that are further away, such as Jupiter and Saturn, but at later times (44). This radiative zone is expected to appear in the outer layers of the planet and to progressively spread over its inner regions (39). In that phase, the evolution of the planet is essentially governed by the ability of the radiative region to transport the still-significant intrinsic heat (the intrinsic luminosity is generally, after a few gigayears, of the same order of magnitude as that of Jupiter: 10^{24} erg s^{-1} to 10^{25} erg s^{-1}). Depending on whether one uses opacities including the presence of grains (45) or opacities that assume that grains are removed by gravitational settling (46), cooling and contraction time scales can differ by factors 2 to 3.

Figure 4 shows typical estimates of model

uncertainties in radii, depending on physical parameters (age and albedo) and input physics (equation of state and opacities). The age of the planetary system (inferred from that of the star) will remain fraught with uncertainty. However, planetary albedos will be determined by either accurate photometry of the eclipsing system or by future direct observations capable of resolving the star-planet system. Theoretical models are also expected to provide better constraints on the albedo (47), but the presence of clouds and grains makes this a complex problem. Hopefully, uncertainties associated with the input physics will be reduced by the calculation of new equations of state that include the latest deuterium compression experiments and by improved opacity calculations. At present, the expected theoretical uncertainty in model radii is about 15% for a $1-M_J$ planet, translating into an accuracy of $\sim 43 M_{\oplus}$ regarding the mass of heavy elements present in the planet. Interestingly enough, this is about the minimal quantity of heavy elements necessary to form such a planet in situ (48). In the case of a $10-M_J$ planet, the fractional uncertainty is smaller, but the absolute precision regarding the mass of heavy elements is $\sim 170 M_{\oplus}$. Systems of planets with small masses at short orbital distances are interesting because they should experience significant mass loss and therefore contain a large proportion of heavy

elements. Radii measurements and corresponding theoretical models would therefore go beyond a simple answer to the question of whether extrasolar giant planets are mainly formed with hydrogen and helium or are mainly rocks and ices [the limiting radius then being on the order of $1/3$ Jupiter radius (R_J) (39)].

Quantity of Heavy Elements and the Formation of Giant Planets

The planets in our solar system formed in the so-called protosolar nebula, a flattened disk of hydrogen, helium, and solid planetesimals (49). Jupiter, Saturn, Uranus, and Neptune are believed to have formed through accretion of a solid core followed by the capture of surrounding gaseous hydrogen and helium (50), but direct gravitational instability of the gas in the disk has been proposed as a mechanism for forming Jupiter and Saturn (51). Saturn's relatively high core mass seems to rule out the latter hypothesis. The extrasolar giant planets discovered so far could have formed by any of these processes. It has been proposed that those at small orbital distances either formed at further distances and then migrated inward (52) or formed in situ within a massive protoplanetary disk (48). An important test of these theories can be provided by a calculation of the quantity of heavy elements captured after the first formation stages.

In our solar system, the first 10 million years after the giant planets reached an appreciable fraction of their current masses were crucial for planetesimal delivery. Between 80 and 90% of the planetesimals that remained in the outer solar system at that time were acquired by the planets or were ejected from the solar system during that period. Dynamic calculations using present-day radii and an initial $50-M_{\oplus}$ disk of planetesimals suggest that less than 2% of the mass of giant planets ($6 M_{\oplus}$ for Jupiter and $2 M_{\oplus}$ for Saturn) is due to late-arriving planetesimals (53). However, at these early epochs, the growing planets possessed effective capture radii that were larger than their present radii (54) and were thus able to capture incoming planetesimals more efficiently while ejecting fewer of them out of the solar system. It is estimated that Jupiter, Saturn, Uranus, and Neptune could have captured by that process up to ~ 17 , 10, 2, and $2 M_{\oplus}$ of heavy elements, respectively (55). Massive extrasolar planets ($\geq 5 M_J$) are able to efficiently eject material out of the system and are therefore expected to acquire a fractionally smaller inventory of "late heavy elements".

Prospects for improving our knowledge of the composition of giant planets and their formation will depend on the following future developments. The calculation of a new hydrogen and helium equation of state consistent with the recent compression experiments is essential. The Cassini orbiter will accurately measure the chemical composition and temperature structure of Saturn's atmosphere (and hopefully of Jupiter as well, although with a lesser accuracy), but it would be cru-

Fig. 3. Predicted effective temperatures and radii (in R_J , $\sim 70,000$ km) of some extrasolar planets and brown dwarfs, including reasonable uncertainties for their mass, albedo, and age (see text) and assuming solar composition. Actual radii could be significantly smaller if the planets contain large proportions of heavy elements. The dashed line is for isolated H-He ($Y = 0.25$) objects after 10 gigayears of evolution. The upper panel also shows potentially important chemical species expected to condense near the photosphere in the indicated range of effective temperatures.

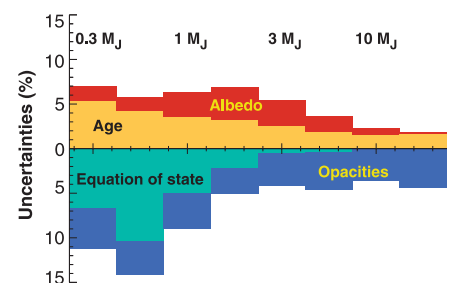
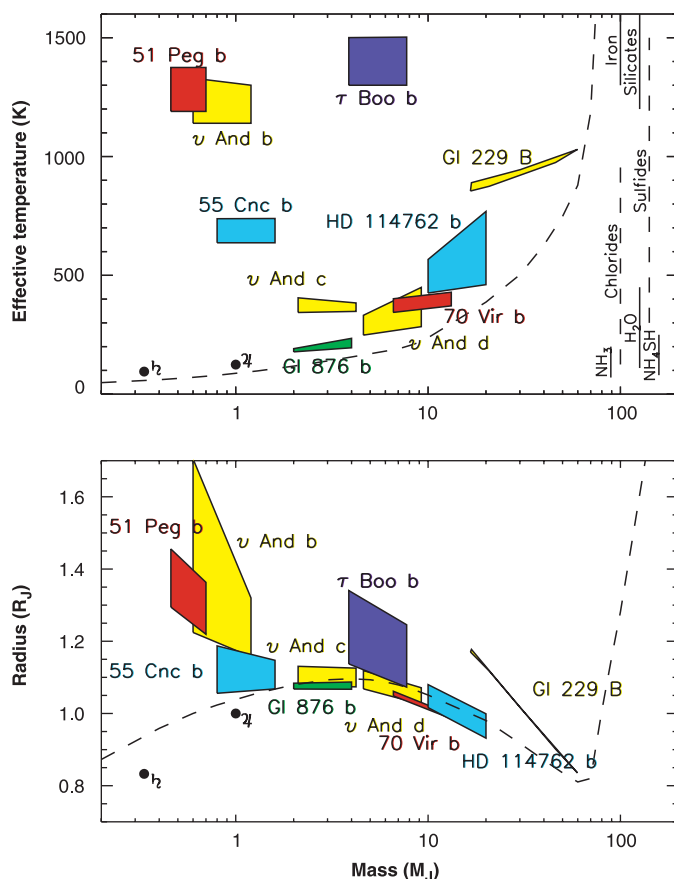


Fig. 4. Fractional uncertainty in radii of extrasolar giant planets (at 0.05 astronomical units from solar-type stars) due to uncertainties in physical parameters (top) and input physics (bottom), as a function of mass. The corresponding absolute uncertainty about the fraction of the planetary mass that is due to heavy elements is directly proportional to the radii uncertainty [a 10% uncertainty in model radii corresponds to a $\sim 9\%$ uncertainty about the mass of heavy elements; that is, in that case and for a $1-M_J$ ($318 M_{\oplus}$) planet, the mass of heavy elements would be known with an accuracy of $\sim 30 M_{\oplus}$]. The albedo was assumed to lie between 0.1 and 0.5; the age between 3 and 7 gigayears.

cial for interior models that the final stages of its orbital tour allow for a better determination of the gravitational moments J_4 and J_6 . Such a measurement could yield constraints on the core mass and abundance of heavy elements in the metallic region that are two to three times stronger (23). A polar Jupiter orbiter would yield an accurate determination of the gravitational field of the planet, including high-order gravitational moments, hence constraining its global composition and dynamic structure (56). Finally, important steps in understanding planet formation will come from spectroscopic measurements of the atmospheres of extrasolar giant planets, and from transit detections that would allow the determination of their radii (57) and hence of the global composition of extrasolar planets.

References and Notes

1. J. K. Campbell and S. P. Synnott, *Astron. J.* **90**, 364 (1985); J. K. Campbell and J. D. Anderson, *ibid.* **97**, 1485 (1989); R. G. French et al., *Icarus* **73**, 349 (1988); W. M. Owen Jr., R. M. Vaughan, S. P. Synnott, *Astron. J.* **101**, 1511 (1991).
 2. R. E. Young, *J. Geophys. Res.* **103**, 22775 (1998).
 3. S. T. Weir, A. C. Mitchell, W. J. Nellis, *Phys. Rev. Lett.* **76**, 1860 (1996); W. J. Nellis, S. T. Weir, A. C. Mitchell, *Phys. Rev. B* **59**, 3434 (1999).
 4. G. W. Collins et al., *Science* **281**, 1179 (1998); G. W. Collins et al., in preparation.
 5. M. Mayor and D. Queloz, *Nature* **378**, 355 (1996); G. W. Marcy and R. P. Butler, *Annu. Rev. Astron. Astrophys.* **36**, 57 (1998).
 6. The term "giant planet" is commonly used for planets more massive than $\sim 10 M_{\oplus}$. Contrary to terrestrial planets, they are expected to contain significant amounts of hydrogen and helium. The distinction between giant planets and brown dwarfs is either through different formation mechanisms (within a protoplanetary disk for giant planets and by fragmentation for brown dwarfs) or through the fact that more massive objects ($M \gtrsim 13 M_J$) burn deuterium whereas lighter ones do not (38).
 7. W. B. Hubbard et al., *Phys. Plasmas* **4**, 2011 (1997).
 8. D. Saumon, G. Chabrier, H. M. Van Horn, *Astrophys. J. Suppl. Ser.* **99**, 713 (1995).
 9. D. Saumon, G. Chabrier, D. J. Wagner, X. Xie, *High Pressure Res.*, in press.
 10. W. R. Magro, D. M. Ceperley, C. Pierleoni, B. Bernu, *Phys. Rev. Lett.* **76**, 1240 (1996).
 11. As discussed by T. Guillot, D. Gautier, and W. B. Hubbard [*Icarus* **130**, 534 (1997)], an estimation of the uncertainty of the density profile is provided by a comparison of two extreme equations of state calculated by Saumon et al. (8). One is thermodynamically consistent and predicts the existence of a first-order phase transition from molecular to metallic hydrogen. The other is continuously interpolated between the low-pressure molecular and high-pressure metallic states.
 12. W. B. Hubbard and M. S. Marley, *Icarus* **78**, 102 (1989); G. Chabrier, D. Saumon, W. B. Hubbard, J. I. Lunine, *Astrophys. J.* **97**, 817 (1992); T. Guillot, G. Chabrier, P. Morel, D. Gautier, *Icarus* **112**, 354 (1994). Five-layer models of Jupiter and Saturn have also been developed by V. N. Zharkov and T. V. Gudkova [*Ann. Geophys.* **9**, 357 (1991)], but this additional complexity is not fully justified.
 13. U. von Zahn, D. M. Hunten, G. Lehmacher, *J. Geophys. Res.* **103**, 22815 (1998). X and Y are the mass mixing ratios of hydrogen and helium, respectively. Previous measurements acquired from the Voyager 2 spacecraft indicated that $Y/(X + Y) = 0.18 \pm 0.04$ [D. Gautier et al., *J. Geophys. Res.* **86**, 8713 (1981)].
 14. J. N. Bahcall and M. H. Pinsonneault, *Rev. Mod. Phys.* **67**, 781 (1995).

15. B. J. Conrath, D. Gautier, R. Hanel, G. Lindal, and A. Marten [*Astrophys. J.* **282**, 807 (1984)] indicate that in Saturn, $Y/(X + Y) = 0.06 \pm 0.05$. However, the discrepancy between the Voyager and Galileo values for Jupiter has cast some doubts on this measurement. The actual helium content may be higher (B. J. Conrath and D. Gautier, in preparation).
 16. E. E. Salpeter, *Astrophys. J. Lett.* **181**, L183 (1973); D. J. Stevenson and E. E. Salpeter, *Astrophys. J. Suppl.* **35**, 221 (1977). Further evidence of the presence of a hydrogen-helium phase separation is the measured depletion of neon (28), thought to dissolve into the falling helium-rich droplets [M. S. Rouston and D. J. Stevenson *Eos* **76**, 343 (1995)].
 17. W. B. Hubbard, in *Origin and Evolution of Planetary and Satellite Atmospheres*, S. K. Atreya, J. B. Pollack, M. S. Matthews, Eds. (Univ. of Arizona Press, Tucson, AZ, 1989), pp. 539–563.
 18. D. J. Stevenson and E. E. Salpeter, *Astrophys. J. Suppl.* **35**, 237 (1977).
 19. D. J. Stevenson, *Annu. Rev. Earth Planet. Sci.* **10**, 257 (1982).
 20. W. B. Hubbard, *Astron. J.* **152**, 745 (1968).
 21. The upper layers [temperature (T) ≤ 2000 K] are not completely homogeneous because of chemical reactions, condensation, and cloud formation. Similarly, at the interface between the core and the metallic hydrogen envelope, an inhomogeneous region might suppress convection. This has few consequences for interior models.
 22. T. Guillot, D. Gautier, G. Chabrier, B. Mosser, *Icarus* **112**, 37 (1994).
 23. T. Guillot, *Planet. Space Sci.*, in press (see <http://xxx.lanl.gov/archive/astro-ph/9907402>).
 24. The microscopic settling velocity of H_2O molecules in the jovian radiative zone is $v_{\text{micro}} \approx 10^{-9} \text{ cm s}^{-1}$. Meridional circulation can be estimated from the Eddington-Sweet formalism, which yields $v_{\text{ES}} \approx 4 \times 10^{-9} \text{ cm s}^{-1}$. Its effect is to oppose the settling of heavy compounds so that in the case of water, for example, the variation in equilibrium abundance should be smaller than 20%. Note that the corresponding time scales are relatively large (the extent of the radiative zone being $\Delta R \approx 4 \times 10^7 \text{ cm}$, on the order of ≈ 0.3 to 1 gigayear. But other mechanisms such as penetrative convection and rotation may be even more effective at rapidly transporting or redistributing heavy elements across the radiative zone [K. Zhang and G. Schubert, *Science* **273**, 941 (1996)].
 25. R. W. Schmitt, *Annu. Rev. Fluid Mech.* **26**, 255 (1994). Salt-finger instabilities (double-diffusive convection) can occur in the ocean where warmer, saltier water overlies colder, fresher water, due to the fact that head conducts through seawater much more rapidly than dissolved salts diffuse. Water and heat are then transported up or down rapidly (but on small scales) through "salt fingers." A similar situation could occur in giant planets with hydrogen instead of water and helium instead of salt.
 26. V. N. Zharkov and V. P. Trubitsyn, *Physics of Planetary Interiors*, W. B. Hubbard, Ed. (Pachart Press, Tucson, AZ, 1978).
 27. W. B. Hubbard et al., *Planet. Space Sci.*, in press (see <http://xxx.lanl.gov/archive/astro-ph/9907402>).
 28. H. B. Niemann et al., *J. Geophys. Res.* **103**, 22831 (1998); W. M. Folkner, R. Woo, S. Nandi, *ibid.*, p. 22847; S. K. Atreya et al., *Planet. Space Sci.*, in press.
 29. A. P. Showman and A. P. Ingersoll, *Icarus* **132**, 205 (1998); M. Roos-Serote et al., *J. Geophys. Res.* **103**, 23023 (1998).
 30. E. Karkoschka and M. G. Tomasko, *Icarus* **97**, 161 (1992); D. Gautier and T. Owen, in *Origin and Evolution of Planetary and Satellite Atmospheres*, S. K. Atreya, J. B. Pollack, M. S. Matthews, Eds. (Univ. of Arizona Press, Tucson, AZ, 1989), pp. 487–512.
 31. G. Wuchterl, T. Guillot, J. J. Lissauer, in *Protostars and Planets IV*, V. Mannings et al., Eds. (Univ. of Arizona Press, in press).
 32. D. Gautier, B. J. Conrath, T. Owen, I. De Pater, S. K. Atreya, in *Neptune and Triton*, D. P. Cruikshank, Ed. (Univ. of Arizona Press, Tucson, AZ 1995), pp. 547–611.
 33. This conclusion is reached by random interior models

of Uranus and Neptune, calculated without any imposed structure [M. S. Marley, P. Gomez, M. Podolak, *J. Geophys. Res.* **100**, 23349 (1995); M. Podolak, J. I. Podolak, M. S. Marley, in preparation].
 34. M. Podolak, W. B. Hubbard, D. J. Stevenson, in *Uranus*, J. T. Bergstrahl, E. D. Miner, M. S. Matthews, Eds. (Univ. of Arizona Press, Tucson, AZ, 1991), pp. 29–61; W. B. Hubbard, J. C. Pearl, M. Podolak, D. J. Stevenson, in *Neptune and Triton*, D. P. Cruikshank, Ed. (Univ. of Arizona Press, Tucson, AZ, 1995), pp. 109–138.
 35. M. Podolak, A. Weizman, M. S. Marley, *Planet. Space Sci.* **43**, 1517 (1995).
 36. W. J. Borucki and A. L. Summers, *Icarus* **58**, 121 (1984); J. Schneider, *C. R. Acad. Sci. Ser. II* **327**, 621 (1999).
 37. D. Saumon et al., *Astrophys. J.* **460**, 993 (1996).
 38. A. Burrows et al., *ibid.* **491**, 856 (1997).
 39. T. Guillot et al., *Astrophys. J. Lett.* **460**, 993 (1996).
 40. The adopted ages vary because they depend on the type of the parent star. For example, I used $t = 1$ to 6 gigayears for 51 Peg, a G2V star, and $t = 1$ to 6 gigayears for *Tau Boötis* and *Upsilon Andromedae*, which are of F7V and F8V type, respectively. See (42) for details.
 41. B. Fegley Jr. and K. Lodders, *Astrophys. J. Lett.* **472**, L37 (1996); A. Burrows and C. M. Sharp, *Astrophys. J.* **512**, 843 (1999).
 42. T. Guillot et al., in *Astronomical and Biochemical Origins and the Search for Life in the Universe*, C. B. Cosmovici, S. Bowyer, D. Werthimer, Eds. (Editrice Compositori, Bologna, Italy, 1997), pp. 343–350.
 43. G. Chabrier and I. Baraffe, *Astron. Astrophys.* **327**, 1039 (1997).
 44. Consider an initially hot planet that progressively cools to an effective temperature close to the equilibrium temperature $T_{\text{eq}} = T_{\text{star}}(R_{\text{star}}/2D)^{1/2}[f(1 - A)]^{1/4}$ (T_{star} and R_{star} are the stellar effective temperature and radius, respectively; D is the orbital distance; A is the Bond albedo of the planet; and f is the phase function). Up to this moment, the interior of the planet had been almost completely convective. But as $T_{\text{eff}}(t) \rightarrow T_{\text{eq}}$, the surface entropy (at the radiative/convective boundary in the atmosphere) s_{surf} and therefore the internal entropy s , also approach a constant value $S(M, t) \approx S_{\text{surf}}(t) \rightarrow S_{\text{eq}}$. The consequence is that in the absence of an additional energy source, the intrinsic luminosity, L , that maintained convective activity drops

$$\frac{dL}{dM} = -T \frac{dS}{dt} \rightarrow 0$$

until a radiative region appears and grows. This allows the internal entropy to continue to decrease (that is, the planet continues to cool and contract beyond the fully convective limit). The appearance of this radiative zone is inevitable, independent of any assumption about opacities.
 45. D. R. Alexander and J. W. Fergusson, *Astrophys. J.* **437**, 879 (1994).
 46. Gaseous Rosseland mean opacities are calculated with opacity data used in M. S. Marley et al., *Science* **272**, 1919 (1996); see (23) for a coarse opacity table.
 47. S. Seager and D. D. Sasselov, *Astrophys. J. Lett.* **502**, L157 (1998); M. S. Marley, C. Gelino, D. Stephens, J. I. Lunine, R. S. Freedman, *Astrophys. J.* **513**, 879 (1999); C. Goukenleuque, B. Bézard, B. Jougnet, E. Lellouch, R. S. Freedman, in preparation.
 48. P. Bodenheimer, O. Hubickyj, J. J. Lissauer, *Icarus*, in press.
 49. J. J. Lissauer, *Annu. Rev. Astron. Astrophys.* **31**, 129 (1993).
 50. J. B. Pollack et al., *Icarus* **124**, 62 (1996).
 51. A. P. Boss, *Astrophys. J.* **503**, 923 (1998).
 52. D. N. C. Lin, P. Bodenheimer, D. C. Richardson, *Nature* **380**, 606 (1996); D. Trilling et al., *Astrophys. J.* **500**, 428 (1998).
 53. J. M. Hahn and R. Malhotra, *Astron. J.* **117**, 3041 (1999).
 54. The effective capture radius is defined as the radius at which an incoming planetesimal on a typical trajectory intercepts more of the gas of the nebula than its own mass. See J. B. Pollack, M. Podolak, P. Bodenheimer, B. Christofferson, *Icarus* **67**, 409 (1986) and (50).

55. T. Guillot and B. Gladman, unpublished data.
 56. W. B. Hubbard, *Icarus* **137**, 196 (1999). See also the proposed NASA discovery mission INSIDE (<http://INSIDEjupiter.lpl.arizona.edu/>).
 57. Two space missions are dedicated to the photometric detection of transits: COROT, a mission of the Centre

National d'Etudes Spatiales, due to be launched in 2003 (<http://www.astrsp-mrs.fr/www/pagecorot/html>); and KEPLER, a NASA project (<http://www.kepler.arc.nasa.gov/>).

58. E. Anders and N. Grevesse, *Geochim. Cosmochim. Acta* **53**, 197 (1989).

59. I thank D. Saumon, B. Gladman, and S. Cazaux for many comments on the manuscript and S. Atreya, D. Gautier, B. Hubbard, A. Morbidelli, T. Owen, and D. Stevenson for stimulating discussions. This research was supported by CNRS (*Action Thématique Innovante* and *Programme National de Planétologie*).

REVIEW

The Galilean Satellites

Adam P. Showman¹ and Renu Malhotra²

NASA's Galileo mission to Jupiter and improved Earth-based observing capabilities have allowed major advances in our understanding of Jupiter's moons Io, Europa, Ganymede, and Callisto over the past few years. Particularly exciting findings include the evidence for internal liquid water oceans in Callisto and Europa, detection of a strong intrinsic magnetic field within Ganymede, discovery of high-temperature silicate volcanism on Io, discovery of tenuous oxygen atmospheres at Europa and Ganymede and a tenuous carbon dioxide atmosphere at Callisto, and detection of condensed oxygen on Ganymede. Modeling of landforms seen at resolutions up to 100 times as high as those of Voyager supports the suggestion that tidal heating has played an important role for Io and Europa.

Jupiter's four large moons, Io, Europa, Ganymede, and Callisto, are collectively known as the Galilean satellites after Galileo Galilei, who discovered them in 1610. Their discovery overturned the Western worldview of an Earth-centered universe. The first quantitative physical studies of these worlds became possible during the 19th century when Simon de Laplace derived the satellite masses from their mutual gravitational perturbations and, subsequently, other workers used a new generation of telescopes (at Yerkes and Lick observatories in the United States) to measure the sizes of these moons. These data yielded estimates of bulk density good to a few tens of percent and revealed the trend of decreasing density from the inner to the outer satellites (Table 1). More recent observations of water ice on the surfaces of the outer three moons led to the inference that the satellite compositions range from mostly silicate rock at Io to 60% silicate rock and 40% volatile ices (by mass) at Ganymede and Callisto (1). This trend probably reflects conditions within the protojovian nebula at the time the satellites formed (2). The Voyager flybys of Jupiter in 1979 revealed evidence of substantial geological activity on these distant worlds (3–6). The observed activity on Io is powered by the tidal distortions of Io's figure caused by the strong gravity of Jupiter, and Europa's fractured terrains also probably result from tidal heating and flexing. Because the rotation rates are synchronized with the

orbital motions, the tides oscillate in amplitude and orientation only because of the satellites' eccentric orbits. The orbital eccentricities of Io, Europa, and Ganymede are excited to nonzero values by resonant gravitational forces between the three satellites (7). In turn, the stability of the resonant orbital configuration (called the Laplace resonance) is controlled by the rate of dissipation of tidal energy within the satellites. Thus, the geologic evolution of these satellites is intimately coupled to their orbital configuration. Embedded within Jupiter's radiation belts, all four satellites are also bombarded by energetic particles that cause chemical reactions and physical erosion that are alien from a terrestrial perspective. These satellites rival the terrestrial planets in complexity but embody processes foreign to our Earth-based experience.

The Galileo spacecraft is performing a 4-year orbital tour scheduled to end in late 1999. By the end of the tour, the spacecraft will have completed over 20 orbits of Jupiter, most arranged to make a close flyby past one of the four Galilean moons. Flyby distances of as little as 200 km have allowed new images with resolution of up to 10 m/pixel to be acquired. (In contrast, Voyager's best resolution was 500 m/pixel.) Qualitatively new constraints have been obtained by a suite of additional experiments: Doppler tracking of the spacecraft's radio signal allowed gravitational moments (hence moments of inertia) to be calculated, a magnetometer provided measurements of the moons' magnetic fields, plasma and energetic particle detectors constrained the electrical and magnetic properties of the moons and their environs, and three spectrometers obtained spatially re-

solved spectra of the moons' surfaces from the ultraviolet to the far infrared (IR) (8). Although the data stream was limited by failure of the high-gain antenna (which, for example, allowed just a few percent of each satellite's surface to be imaged at resolutions exceeding 200 m/pixel), the nature of the data sets is so unique that the measurements have boosted our understanding and raised numerous new questions. Concurrently, observations from ground-based facilities and the Earth-orbiting Hubble Space Telescope (HST) have yielded important discoveries.

Callisto

Unlike Io, Europa, and Ganymede, Voyager showed Callisto to be a heavily cratered body apparently devoid of endogenic volcanic or tectonic landforms (6). Primary interest in Callisto has centered on comparison with Ganymede, which has similar bulk properties but a highly tectonized surface. Callisto's mean density suggests roughly equal masses of rock and ice, but early opinions differed about whether the interior contained a primordial, undifferentiated mixture of the two components or a differentiated ice mantle overlying a silicate rock and iron core (1, 5). Callistan craters are flatter (and often display a distinctive morphology) compared with their terrestrial counterparts, indicating that the uppermost 10 km is mechanically dominated by ice rather than rock (9, 10), supporting the idea of at least partial differentiation of Callisto's interior. IR spectra of the surface contain numerous water ice absorption features, but the low albedo and existence of other nonice features (11) imply contamination by darker material. Radiative transfer retrievals of the spectra have yielded mean ice mass fractions of the uppermost ~1 mm ranging from 10 to ~50%, with some regions recognized as essentially ice free (5, 12, 13).

Interior structure and magnetic field. From Galileo tracking data, Callisto's moment of inertia has been determined to be $C/MR^2 = 0.359 \pm 0.005$, which is 4 standard deviations less than 0.38, the value expected for a homogeneous rock and ice body of Callisto's mass and radius (14). Three-layer interior models suggest the existence of a central silicate core up to 50% of Callisto's

¹Department of Mechanical Engineering, University of Louisville, 215 Sackett Hall, Louisville, KY 40292, USA. E-mail: showman@flolab.spd.louisville.edu ²Lunar and Planetary Institute, 3600 Bay Area Blvd., Houston, TX 77058, USA. E-mail: renu@lpi.jsc.nasa.gov